

A New Method to Reconstruct the Energy and Determine the Composition of Cosmic Rays from the Measurement of Cherenkov Light and Particle Densities in Extended Air Showers[¶]

A. Lindner, *Uni. Hamburg, II. Inst.f.Exp.Physik,
Luruper Chaussee 149, D-22761 Hamburg, Germany, E-Mail: lindner@mail.desy.de*

Abstract

A Monte-Carlo study is presented using ground based measurements of the electromagnetic part of showers initiated in the atmosphere by high energetic cosmic rays to reconstruct energy and mass of primary particles with energies above 300 TeV. With two detector arrays measuring the Cherenkov light and the particle densities as realized in the HEGRA experiment the distance to the shower maximum and the lateral development of air showers can be coarsely inferred. The measurable shower properties are interpreted to determine energy and energy per nucleon of the primary particle.

1 Introduction

This paper describes a new method to derive the elemental composition and the energy spectrum of cosmic rays for energies above a few hundred TeV from measurements of Cherenkov light and particle densities at ground level. The main idea is to determine the distance between the detector and the shower maximum, which is used to correct experimental observables for fluctuations in the shower developments. The depth of the shower maximum itself turns out to be a coarse measurement of the energy per nucleon of the nucleus hitting the atmosphere. The paper is organized as follows:

After describing the experimental observables which will be used to reconstruct characteristics of the primary particle, the event simulation is sketched and features of the longitudinal and lateral shower development in the atmosphere are considered. The following three sections deal with reconstruction of the position of the shower maximum, of the energy per nucleon and of the primary energy. Finally methods to determine the chemical composition are described followed by the summary and conclusions.

2 The Experiment and Observables

Although the method described in this paper was developed primarily for the HEGRA experiment it can equally well be applied to any installation registering Cherenkov light and charged particles of extended air showers (EAS). The method can be easily generalized to all experimental setups which allow the determination of the distance to the shower maximum. However some properties of the HEGRA experiment need to be mentioned to understand details discussed in the following sections.

[¶]Summary of two talks given at the *XVth Cracow Summer School of Cosmology, Lodz, 1996*

The experiment HEGRA is a multi-component detector system described in detail elsewhere [1] for the measurement of extended air showers (EAS). At a height of 2200 m a.s.l. it covers an area of 180-180 m². In this paper only the scintillator array of 245 huts with a grid spacing of 15 m including denser part near the center and the so called AIROBICC array of 72 open photomultipliers measuring the Cherenkov light of air showers on a grid with 30 m spacing also with a central concentration, are used. The energy threshold (demanding a signal from at least 14 scintillator or 6 AIROBICC huts) lies at 20 TeV for proton and 80 TeV for iron induced showers.

The measured particle density in the plane perpendicular to the shower axis is fitted by the NKG formula [2]. In the fit a fixed Moliere radius of 112 m is used. The shape parameter *age* and the integral number of particles *Ne* result from the fitting procedure. As the HEGRA scintillators are covered with 5 mm of lead (which suppresses the detection of low energy electrons but allows the measurement of photons after pair production in the lead) the values obtained for *age* and *Ne* cannot be compared to simple expectations from the cascade theory: *age* maybe smaller than 1 although the measurement takes place well behind the shower maximum while the shower size *Ne* is generally larger than for measurements without lead on the scintillator detectors.

The Cherenkov light density is only analyzed in the interval 20 m < r < 100 m from the shower core due to technical reasons although HEGRA in principle could sample the Cherenkov light density up to 200 m. In the range between 20 and 100 m the Cherenkov light density can be well described by an exponential

$$\rho_C(r) = a \cdot \exp(r \cdot slope). \quad (1)$$

As in the NKG fit two parameters are obtained from the analysis of the Cherenkov light: the shape parameter *slope* and the total number of Cherenkov photons reaching the detector level between 20 and 100 m core distance $L(20-100)$.

3 Simulation

EAS in the energy range from 300 TeV to 10 PeV were simulated using the code CORSIKA 4.01 [3]. The model parameters of CORSIKA were used with their default values and the fragmentation parameter was set to “complete fragmentation”. This results in a complete disintegration of the nucleus after the first interaction. Showers induced by the primary proton, α , oxygen and iron nuclei were calculated.

The number of generated Cherenkov photons corresponds to a wavelength interval of [340 – 550 nm]. In the main this paper assumes perfect measurements of the number of particles and Cherenkov photons and a perfect shower core determination in order to concentrate on the physical principles and limitations of the methods to be described. To study the influence of the realistic experimental performance the events were passed through a carefully checked detector simulation [4] (performed with measured response functions) and reconstructed with the same program as applied to real data. Here each event was used 20 times to simulate different core positions inside and impact points outside the experimental area, which nevertheless fire sufficient huts of the arrays to fulfill the trigger conditions.

In total 1168 events were generated with CORSIKA 4.01 with zenith angles of 0,15,25 and 35° at discrete energies between 300 TeV and 10 PeV.

4 The Development of Showers in the Atmosphere

Some basic characteristics of the EAS simulated with CORSIKA 4.01 are summarized here. Features independent or sensitive to the mass of the nucleus hitting the atmosphere are described. These will allow the reconstruction of primary energy and mass from the observables mentioned above.

4.1 The longitudinal Shower Development

Shown on the left of Figure 1 are the mean longitudinal developments of 300 TeV proton and iron induced air showers, where electrons and positrons above an energy of 3 MeV were counted. This will be subsequently called, the shape of the longitudinal shower development. For each shower the maximum (defined as the point in the shower development with the maximal number of particles) was shifted to zero before averaging. Afterwards the mean distribution was normalized to the mean particle number at the shower maximum. Concerning the shape of the longitudinal development behind the shower maximum

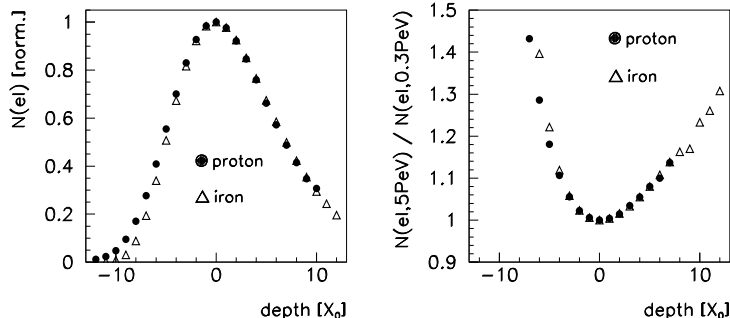


Figure 1: Left: the mean longitudinal development of 300 TeV p and Fe showers normalized to the number of particles in the maximum. The depth of each shower maximum was shifted to $0 X_0$. Right: the mean longitudinal development for 5 PeV showers divided by the mean development for 300 TeV showers (normalized at the shower maximum at $0 X_0$).

no systematic differences depending on the primary particle are visible. The right plot in Figure 1 shows the change in the longitudinal development with increasing primary energy. The shapes broaden independently of the primary particle. Both plots may be explained by a lucky combination of two effects:

1. As visible from simulated proton showers at 300 TeV and 5 PeV the longitudinal shower shape gets broader with increasing energy.
2. After the first interaction an iron induced shower can be described as a superposition of nucleon induced subshowers. Each of them have different subshower maxima fluctuating around a mean value. To achieve the distributions in Figure 1 the maxima of the whole EAS (and not the maxima of the subshowers) were overlaid. Therefore a Fe shower appears to be broader than a proton shower of the same energy per nucleon.

In CORSIKA 4.01 (other simulations have to be tested) both effects combine in such a way that the longitudinal shape of the EAS behind the maximum becomes independent

of the mass of the primary nucleon for the same primary energy. The mean atmospheric depths of the maxima depend on the energy per nucleon E/A (see section 6) and are subjected to large fluctuations. Figure 2 shows the corresponding correlation: the column density traversed by a shower up to its maximum, named depth of maximum in the following (calculable from the distance and the zenith angle), is correlated with E/A for all different simulated primaries from p to Fe and all zenith angles. With

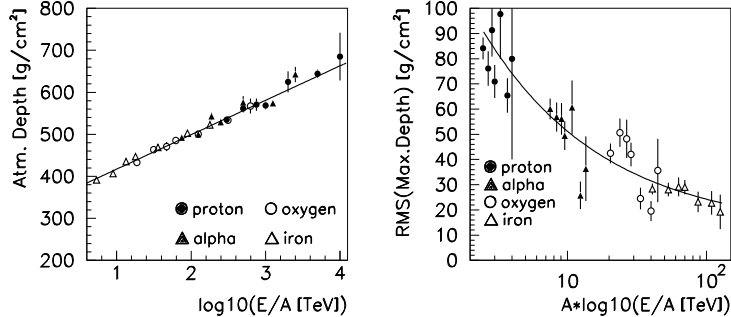


Figure 2: Left: the mean atmospheric depth of the shower maxima as a function of energy per nucleon. The line shows a fit to the correlation. Right: as an attempt to illustrate the origin of the fluctuations (rms) of the atmospheric depth of the shower maxima they are plotted as a function of energy E and nucleon number A . The line shows a fit to the correlation.

the “complete fragmentation” option in our simulations the correlation follows a linear function. From Figure 2 an elongation rate of approximately $82 \text{ g/cm}^2 / \log_{10}(E/E_0)$ is derived:

$$\text{depth}(\text{max}) = \left[(335 \pm 3) + (82 \pm 2) \cdot \log_{10} \left(\frac{E/A}{\text{TeV}} \right) \right] \text{ g/cm}^2. \quad (2)$$

If the depth of the shower maximum is measured the energy per nucleon E/A can be inferred. Due to statistical fluctuations in the shower development and therefore in the depth of the shower maximum (Figure 2) the resolution for E/A is modest. The spread decreases with increasing nucleon number A as the EAS of a complex nucleus consists of many overlapping nucleon induced subshowers so that the whole EAS exhibits less fluctuations than the individual subshowers. The resolution improves slightly also with rising E/A because more interactions take place until the shower maximum is reached. Figure 2 (right) shows a parameterization of the fluctuations of the depth of the shower maxima.

It is interesting to note that for a specific primary particle and energy the number of particles in the shower maximum $N_e(\text{max})$ is independent of the depth of the maximum. Therefore this number differs between proton and iron induced showers of the same primary energy even if the shower maxima are accidentally at the same position.

The most important characteristics of the longitudinal shower development discussed above and which will be used for the reconstruction of primary energy and mass in the next sections are:

- The longitudinal shower development behind the shower maximum does not depend on the mass of the primary particle and only slightly on the primary energy.
- The mean depth of the shower maximum is determined only by the energy per nucleon E/A .

- Fluctuations in the position of the shower maximum decrease with increasing nucleon number and slightly with increasing energy.

4.2 The lateral Shower Development

In hadronic interactions the typical transverse momentum stays roughly constant with energy. Therefore the lateral spread of hadronic showers should decrease with increasing energy per nucleon as the ratio of transverse to longitudinal momentum gets smaller in the early part of the shower development where the energies of the interacting particles are still comparable to the primary energy. In principle this effect could be measured for a known distance to the shower maximum i.e. by comparing the number of Cherenkov photons reaching the detector level relatively close to the core with the number of all photons detectable at the ground level or by analyzing *age*. In this way a separation of heavy and light primaries turns out to be possible at energies below 1 PeV. At energies in the knee region nearly no differences between proton and iron showers remain. Obviously here E/A even for iron showers becomes so large that any influence of the hadronic transverse momentum is washed out and the lateral shape of the shower is dominated by scattering processes and interactions of particles of relatively low energies in the later part of the shower development.

5 Reconstruction of the Position of the Shower Maximum

This section deals with the reconstruction of the distance between the shower maximum and the detector. It can be determined from the shape of the lateral Cherenkov light density (*slope*) and in principle also from the shape parameter *age* of the particle distribution at detector level.

As already noticed by Patterson and Hillas [5] for showers with energies above 1 PeV the distance between the detector and the maximum of an EAS can be inferred from the lateral distribution of the Cherenkov light within about 100 m core distance. This is possible, because Cherenkov light emitted at a specific height shows a specific lateral distribution at detector level. The light from the early part of the shower development, where the energies of the particles are still very high so that scattering angles are very small, is concentrated near 120 m (the so called Cherenkov ring). Cherenkov light produced closer to the detector level hits the ground closer to the shower core. The measurable Cherenkov light density of one EAS is the sum of all contributions from all heights, where lateral distributions from different heights enter with amplitudes corresponding to the number of Cherenkov light emitting particles in the different heights. Hence the shape of the measurable lateral light density distribution depends on the longitudinal shower development. If the shower maximum approaches the observation level more light is produced close to the detector reaching the ground near the shower core. Consequently the lateral Cherenkov light density in the range up to 100 m core distance drops the steeper the closer the shower maximum approaches the detector.

In Figure 3 the correlation between the distance to the shower maximum and the parameter *slope* derived from the Cherenkov light distribution is plotted for different primary nuclei and zenith angles up to 35 degree for primary energies of 0.3 and 5 PeV. The distance to the shower maximum can be accurately determined from *slope* independent of

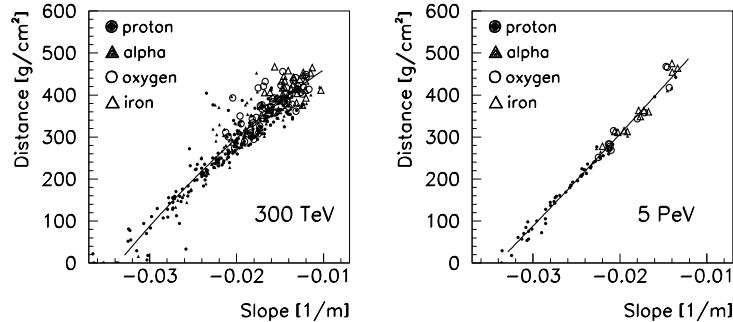


Figure 3: The distance between detector and shower maxima plotted against the parameter *slope* for 300 TeV (left) and 5 PeV (right) primary energy. The lines show fits to the correlations.

the type of the primary particle and zenith angle* The correlation between distance and *slope* depends slightly on the primary energy due to the changing longitudinal shower development. Figure 3 shows simple polynomial fits describing the correlation rather well. The dependence of the fit parameters on $\log(E)$ were again parameterized with polynomials resulting in a two dimensional function of *slope* and $\log(E)$ to determine the distance to the shower maximum. The systematic uncertainties in the reconstruction of the distances depending on particle type or primary energy are less than 5% increasing a little for zenith angles of 35° . Such a systematic error for large zenith angles is expected as these showers develop longer at high altitude where the threshold energy for electrons to produce Cherenkov light is higher than for showers with vertical incidence.

Two shower properties contribute to the accuracy of the determination of the shower maximum. For a given primary energy the resolution improves with decreasing distance between detector and shower maximum and with increasing number of nucleons. Accidentally both contributions behave in such a manner that for fixed zenith angle and primary energy the resolution becomes independent of the mass of the primary particle within the statistical errors of the event sample. Corresponding results are plotted in Figure 4. The right part of Figure 4 shows the reason for the finite resolution of the distance determination with *slope*. Showers, where the distance is underestimated, do not decay as fast as an average shower behind the shower maximum. Consequently *slope* is smaller than expected and the distance is reconstructed too small. Showers with overestimated distances exhibit a shorter longitudinal extension behind the shower maximum. It is interesting to note that the length of the shower behind the maximum is anti correlated with the number of particles in the maximum: the faster the decay after the maximum the more particles arise in the maximum.

It is worthwhile to note that other approaches, like the reconstruction of the shower maximum from measurements of the time profile of the Cherenkov light pulses at core distance beyond 150 m [4] show different limitations as different shower properties than with *slope* are measured. In principle it is also possible to determine the distance to the shower maximum with *age*, but the experimental resolution of an *age* measurement cannot compete with a *slope* determination. An improvement is only possible with a much denser coverage with active detector components than in present experiments (typically around 1%). In addition *age* depends on the primary particle type so that an unbiased measurement of

*neglecting atmospheric absorption

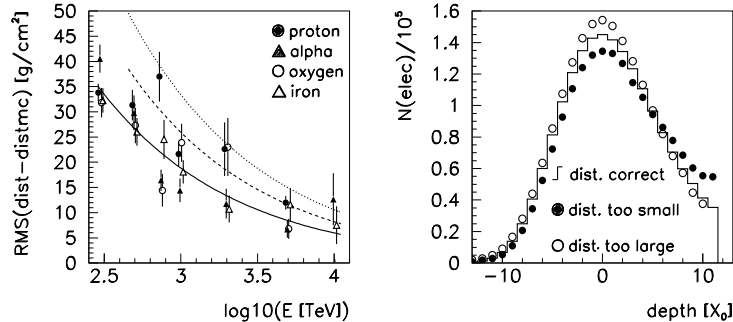


Figure 4: Left: the rms value of the distributions of the absolute difference between reconstructed and MC generated distance to the shower maximum for zenith angles of 0° and 15° . The line shows a fit to the correlation. The broken and dotted lines indicate fits to simulated events at zenith angles of 25° and 35° respectively.

Right: the mean longitudinal development of 300 TeV proton showers where the reconstructed distance is more than 20 g/cm^2 too large (open dots), too small (full dots) or correct within 10 g/cm^2 (line). The maximum for each individual shower was shifted to zero before averaging. In contrast to Figure 1 the distributions were not normalized to the number of particles in the maximum.

the position of the shower maximum is not possible at energies below 1 PeV.

6 Determination of Energy per Nucleon E/A

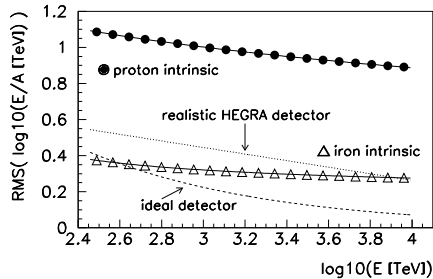


Figure 5: Different contributions to the accuracy of the E/A reconstruction with *slope* and zenith angle: “intrinsic” contributions refer to Figure 2 showing the fluctuations in the shower development. The broken line (“ideal detector”) displays the principal accuracy limit achievable with the method to reconstruct the distance to the shower maximum with *slope*, the dotted line shows the corresponding accuracy including the realistic performance of the present HEGRA detector (both for 0° and 15° zenith angle).

With known distance to the shower maximum and known zenith angle the penetration depth of the shower into the atmosphere until it reaches the maximum can be inferred. E/A can be estimated using the correlation shown in Figure 2. The resolution for E/A is limited by the natural fluctuations of the shower maxima positions (Figure 2) and by principle accuracy limits of the *slope* method (Figure 4). Of course further experimental errors may contribute in addition. In Figure 5 the different contributions (to be added quadratically) are compared. The uncertainty for proton induced showers is always dominated by statistical fluctuations of the shower developments, whereas for iron showers at low energies the intrinsic uncertainty of the *slope* method contributes significantly.

At energies around the “knee” the accuracy is always limited by variations of the shower developments.

7 Reconstruction of primary Energy

With a HEGRA type of detector two different methods may be used to reconstruct the primary energy:

1. Interpreting the shower size at detector level measured by the scintillator array corresponds to a determination of the leakage out of the “atmospheric calorimeter”. These “tailcatcher” data allow for an accurate energy reconstruction if combined with information on the shower development. This ansatz can be applied as the shape of the longitudinal development behind the shower maximum does not depend on the primary particle (see section 4.1) and the distance to the shower maximum can be measured independently of the mass of the primary nucleus.
2. The measurement of the amount of Cherenkov light makes use of the atmosphere as a fully active calorimeter. Although in principle superior to the “tailcatcher” approach this idea suffers from the large extension of the Cherenkov light pool. Depending on the distance to the shower maximum only 20 to 55% of all Cherenkov photons reach the detector within 100m core distance. In contrast to this the particle density drops very fast with increasing distance to the shower core so that a detector of the HEGRA size is sufficient to determine the number of all particles reaching the ground level.

Both algorithms described in the present paper can roughly be divided into two steps: first the distance of the shower maximum to the detector (derived from the shape of the lateral Cherenkov light density distribution) is used to correct for different longitudinal shower developments. As only experimental quantities measuring the electromagnetic part of the air shower are considered here it follows naturally, that only the energy deposited in the electromagnetic cascade can be reconstructed directly. In a second step a correction for the non measured energy has to be performed. This correction depends on E/A only, which is determined from the depth of the shower maximum as described in the previous section.

The following plots and parameterizations only take into account showers which reach their maximum at least 50 g/cm^2 above the detector, because otherwise one can hardly decide whether a shower reaches its maximum above detector level at all. The treatment of showers arriving at detector level before reaching their maximum has to be considered separately.

7.1 Energy Reconstruction from Particle and Cherenkov Light Measurement

In this section the primary energy will be reconstructed in the following manner:

1. With the known distance to the shower maximum the number of particles in the shower maximum $N_e(\text{max})$ is derived from the measurement at detector level N_e .
2. $N_e(\text{max})$ is proportional to the energy deposited in the electromagnetic cascade.
3. From the energy per nucleon E/A and $N_e(\text{max})$ the total primary energy is inferred.

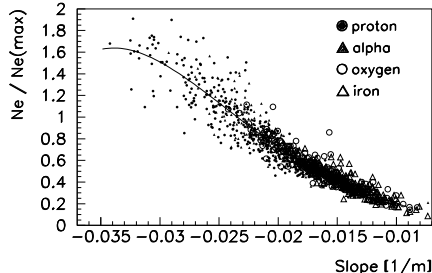


Figure 6: The ratio of Ne (measured below 0.5 cm of lead) and the number of particles at the maximum $Ne(\max)$ as a function of $slope$. The line shows a fit to the correlation.

systematic uncertainties in the energy reconstruction originate from the lead coverage. Due to the conversion of photons in the lead the measured number of particles is larger than $Ne(\max)$ for showers reaching their maximum close to the detector. In Figure 6 the ratio of Ne to $Ne(\max)$ is correlated with $slope$ measuring the distance between detector and shower maximum. Using $slope$ in this correlation instead of the distance permits the handling of all energies in one correlation:

$\xi_{\text{dis}}(slope)$ is applied to determine $Ne(\max)$ from the observed Ne at detector level and from $slope$ measuring the distance to the shower maximum.

No change of the correlation for different primary energies was observed (compare table 1 and the related discussion in the text). No systematic differences between different primary particles are visible. In the second step the primary energy is determined from $Ne(\max)$ and E/A . Two sub steps are necessary here: first the energy contained in the electromagnetic part of the EAS has to be derived, followed by an E/A dependent correction to determine the primary energy. The electromagnetic energy is proportional to $Ne(\max)$ for a fixed shape of the longitudinal shower development. Because the shape changes slightly with primary energy E both $Ne(\max)$ and E are necessary to determine the electromagnetic energy. During our simulations the total amount of electromagnetic energy in an EAS (defined as the sum of all π^0 energies) was not recorded so that the ratio of electromagnetic energy to the primary energy and the ratio of $Ne(\max)$ to the electromagnetic energy could not be calculated directly for the simulated events. Hence arbitrary factors may be multiplied to the two correction functions below as long as their product is kept constant. The functions are:

$\xi_{\text{lon}}(E)$ takes into account the change of the longitudinal shower development with E .

$\xi_{\text{em}}(E/A)$ is used to correct from the electromagnetic energy to the total energy E of the primary nucleus and will be discussed a little more detailed.

The fraction of the primary energy which goes into the electromagnetic part of the shower rises with increasing energy as the probability for hadrons to perform subsequent interaction with the production of additional neutral pions increases with the hadron energy. For a nucleus the fraction of the electromagnetic energy should depend only on E/A . Following the results of [6] a function was fitted to the correlation of $Ne(\max)/E$ with E/A using the generated MC events:

$$\xi_{\text{em}}(E/A) = \frac{Ne(\max)}{E \cdot \xi_{\text{lon}}(E)} = \left[1 - \left(\frac{E/A}{33 \text{ GeV}} \right)^{-0.181} \right] \text{TeV}^{-1}. \quad (3)$$

The first step for reconstructing the primary energy is the determination of $Ne(\max)$ from the observables Ne and $slope$. As the scintillator huts of the HEGRA experiment are covered with $1 X_0$ of lead the total number of particles is not measured directly. In simulations the ratio of measured particles and the number of particles before the lead was found to depend only on the distance to the shower maximum but not on primary energy nor on the nucleon number of the primary particle. Therefore no systematic

The ratio of this correction for protons to iron at 300 TeV amounts to 1.34 decreasing to 1.16 at 5 PeV. The difference between proton and iron showers is larger than derived by extrapolating the results in [6] to the mean atomic number of air because the fraction of the total energy deposited in the electromagnetic cascade is different in air showers compared to showers developing in solid state calorimeters: in air the interaction length for charged pions is comparable to their decay length so that the competition between pion decay and secondary interaction with subsequent production of neutral pions (feeding the em. cascade by their decay to two photons) lowers the fraction of energy deposited in the electromagnetic cascade. Now the primary energy is calculable by

$$E = \frac{Ne(\max)}{\xi_{\text{lon}} \cdot \xi_{\text{em}}} = \frac{Ne}{\xi_{\text{dis}} \cdot \xi_{\text{lon}} \cdot \xi_{\text{em}}} \quad . \quad (4)$$

Due to the energy dependence of the correlation between *slope* and distance to the maximum and of $Ne(\max)/E$ (both due to a slightly changing shape of the longitudinal shower development) energy and distance to the shower maximum cannot strictly be determined separately but have to be calculated iteratively. However the energy dependencies are small. Therefore in the calculation as a start value a parameterization of the correlation of distance and *slope* neglecting any energy dependence is used to derive a first distance value. With this an energy estimation is calculated and with this energy a new distance. This distance in turn gives a new energy value again. After two iterations usually neither the distance nor the energy results change further.

The application of the whole procedure to simulated events results in systematic uncertainties on the order of 5%. Several contributions to the energy resolution for iron and proton showers are listed in table 1. For 300 TeV iron showers most of the uncertainties

Method	Fe 300 TeV	Fe 5 PeV	Prot. 300 TeV	Prot. 5 PeV
Ne(max)	(6 ± 1)%	(4 ± 1)%	(15 ± 1)%	(9 ± 1)%
Ne at detector, dist. from MC	(12 ± 1)%	(6 ± 2)%	(17 ± 1)%	(7 ± 1)%
Ne from fit, dist. from MC	(20 ± 2)%	(7 ± 2)%	(18 ± 1)%	(11 ± 2)%
Ne, <i>slope</i> from fits, E/A from MC	(22 ± 2)%	(7 ± 2)%	(15 ± 1)%	(11 ± 2)%
Ne, <i>slope</i> from fits, E/A reconstr.	(31 ± 3)%	(12 ± 4)%	(25 ± 2)%	(11 ± 2)%

Table 1: Rms values of different quantities contributing to the energy resolution which can be achieved with the method using *Ne* and *slope*. In the first two rows the identity of the primary particle is used from the simulations. “Ne(max)”, “Ne at detector” and “dist” are MC quantities, *Ne* and *slope* experimental observables. E/A denotes the energy per nucleon, which in the last line of the table is reconstructed from *slope* and the zenith angle.

stem from the NKG fit to the scintillator data with subsequent fluctuations in *Ne* and from a modest resolution for E/A (compare Figure 5). At 300 TeV the ratio of reconstructed to generated energy exhibits a tail to large values which originates from the large uncertainties in the determination of E/A and the relatively large corrections depending

on E/A as shown in equation 3. Already at an energy of 500 TeV the tail to high energies nearly disappears resulting in a rms value of 20%. For energies of 1 PeV and larger the resolution amounts to roughly 10%. The much improved energy resolution is achieved due to better Ne and E/A determinations and a smaller correction depending on E/A . The energy resolution for proton showers improves from 25% at 300 TeV to about 10% at 5 PeV. Even a direct measurement of $Ne(\max)$ and an unambiguous identification of its mass would not improve the energy resolution very much compared to the reconstruction using only experimental observables.

7.2 Energy Reconstruction from Cherenkov Light alone

As in the previous section the energy can be reconstructed by replacing Ne by $L(20-100)$. The fraction of the Cherenkov light in the interval from 20 to 100 m depends on the distance to the shower maximum (geometry) and on E/A , because the lateral spread of an EAS decreases with decreasing ratio of transverse to longitudinal momentum in the interactions. The following effects were taken into account for the energy reconstruction with Cherenkov light only:

$\zeta_{\text{dis}}(\text{slope}, \mathbf{E})$: The fraction of light contained in $L(20-100)$ depends on the distance to the shower maximum. Due to the differences in the longitudinal shower development an additional small energy dependence was also taken into account (corresponding to ξ_{dis} and ξ_{lon} of the previous section).

$\zeta_{\text{em}}(\mathbf{E}/\mathbf{A})$: For a given distance the fraction in $L(20-100)$ depends on E/A also. As in the previous section ($\xi_{\text{em}}(\mathbf{E}/\mathbf{A})$) this originates from the energy fraction deposited in the electromagnetic cascade of an EAS, but the lateral extension of the Cherenkov light pool also contributes.

$\zeta_{\text{den}}(\text{height})$: The threshold for electrons to produce Cherenkov light varies from 38 MeV at a height of 300 g/cm² to 21 MeV at the detector level of 793 g/cm². Therefore the amount of Cherenkov light generated in the atmosphere depends on the height of the shower maximum.

The correction depending on energy per nucleon is given explicitly below.

$$\zeta_{\text{em}}(\mathbf{E}/\mathbf{A}) = \frac{L(20-100)/1.3 \cdot 10^7}{E \cdot \zeta_{\text{dis}} \cdot \zeta_{\text{den}}} = \left[1 - \left(\frac{E/A}{178 \text{ GeV}} \right)^{-0.180} \right] \text{TeV}^{-1}. \quad (5)$$

This correction is larger than equation 3 because of the correction for the Cherenkov light beyond 100 m distance. The remaining systematic uncertainties after all corrections for different primary particles, energies and zenith angles are less than 10%, a little worse compared to the energy reconstruction with Ne . The reasons are the larger E/A dependencies. The energy resolution ranges from 45% (35%) at 300 TeV to 8% (11%) at 5 PeV for iron (proton) induced showers.

7.3 Comparison of both Energy Reconstructions

Assuming perfect detectors the light in the interval from 20 to 100 m core distance can be reconstructed with an error smaller than 1%. Clearly this is superior to the measurement of Ne . However the obtainable energy resolution at low energies is limited by uncertainties in the distance and E/A reconstruction. In spite of the accurate measurement of the Cherenkov light the final resolution at 300 TeV is even worse than using Ne

mainly because the correction depending on E/A is larger. At high energies fluctuations in the shower development concerning its shape and the fraction of energy deposited in the electromagnetic cascade limit the energy resolution, which could only be improved by an accurate determination of the non electromagnetic component. It should be noted however that energy resolutions around 10% as obtained here for 5 PeV are already much better than needed for most applications.

The energy resolutions for both methods suffer mainly from the same uncertainties in distance and E/A determination. Therefore no significant improvement can be obtained by combining both measurements. However the two methods to determine the primary energy are not equally sensitive to experimental errors. For example the energy reconstructed with Cherenkov light only is much less influenced by faulty *slope* measurements than the reconstruction with Ne . Assuming that the light density at 100 m distance from the shower core is measured correctly while *slope* is reconstructed incorrect, the energy determined with Ne is incorrect by nearly a factor of two if *slope* is changed by 20% whereas the energy derived from Cherenkov light only is shifted by less than 10%. This different behavior is explained by the fact, that a too large (small) *slope* leads to too small (large) corrections ξ_{dis} and ζ_{dis} , but in addition too large (small) *slopes* give too small (large) values for $L(20-100)$ partly compensating the effect of the wrong ζ_{dis} correction.

8 Determining the Chemical Composition

With the reconstruction of the shower development described in the previous section not only the energy is inferred independently of the mass of the primary nucleus but also the nucleon number of the hadron hitting the atmosphere can be determined coarsely by only measuring the electromagnetic part of the EAS. In the following sections first the energy per nucleon derived from the longitudinal shower development and then the properties of the lateral shower extensions will be analyzed for their sensitivity on the nucleon number of the primary particle. The third section combines all information concerning the chemical composition deduced here from the four observables Ne , *age*, *slope* and $L(20-100)$ for 300 TeV showers as an example.

8.1 The Nucleon Number from the longitudinal Shower Development

With procedures to determine the primary energy and an estimation of the energy per nucleon E/A from the position of the shower maximum as described in section 6 it is straightforward to calculate the nucleon number:

$$\log_{10}(A) \equiv \log_{10} \left(\frac{\text{energy}}{\text{energy/nucleon}} \right). \quad (6)$$

Figure 7 displays the reconstructed $\log_{10}(A)$ values for proton and iron showers of 0.3 and 5 PeV. The other primaries were omitted in order to keep a clear picture. Further results are summarized in table 2. The reconstructed mean values correspond within statistical errors to the expectation values. For the energy reconstruction the method with Ne was used, but the same results are obtained with the second method of determining the primary energy.

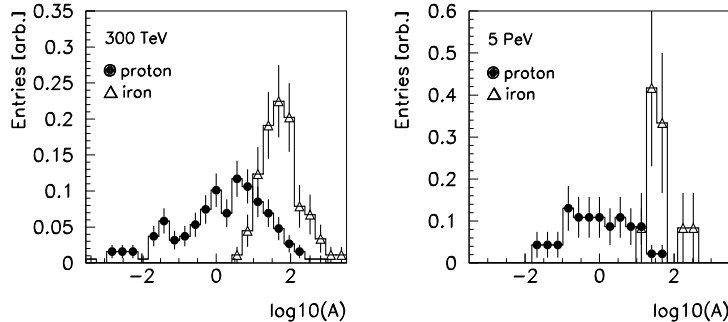


Figure 7: The reconstructed nucleon number for proton and iron primaries of 300 TeV (left) and 5 PeV (right).

Primary	$\log_{10}(A)$				
	Mean	RMS 300 TeV	RMS MC	RMS 5 PeV	RMS MC
Proton	0.00	1.19 ± 0.09	1.00 ± 0.07	0.82 ± 0.13	0.77 ± 0.12
Helium	0.60	0.83 ± 0.08	0.70 ± 0.07	0.42 ± 0.12	0.30 ± 0.09
Oxygen	1.20	0.63 ± 0.08	0.52 ± 0.07	0.26 ± 0.08	0.22 ± 0.06
Iron	1.75	0.53 ± 0.06	0.35 ± 0.04	0.38 ± 0.11	0.29 ± 0.09

Table 2: The mean and rms values of the distributions of the reconstructed $\log_{10}(A)$ values. “MC” symbolizes the result obtained by using the generated MC energy and the depth of the shower maximum directly from MC. The numbers given in the “MC” columns therefore show the contributions from fluctuations in the longitudinal shower development only. Differences to the fits shown in Figure 5 originate from the summation over all zenith angles in this table.

Light and heavy primaries can be distinguished by their different mean values and by their different spreads. The spread of the $\log_{10}(A)$ distributions is dominated by the statistical fluctuations of the depth of the shower maximum with subsequent uncertainties in the E/A determination (see Figures 2 and 5). Even a perfect energy determination would hardly improve the separation of different primary particles.

8.2 Composition Analysis from the lateral Shower Development

In section 4.2 differences concerning observable lateral extensions of EAS which depend on E/A have been touched briefly. Age can be used to estimate E/A if the energy of the primary particle and the distance to the shower maximum is known. Figure 8 (left) compares age for different primaries of 300 TeV energy. To use this discrimination the expectation value of age for proton induced showers was parameterized:

$$age(p) = 1.42 - 0.10 \cdot \log_{10}(E/\text{TeV}) + 18.0 \cdot slope . \quad (7)$$

For each reconstructed shower the actual age is then compared to the expectation for primary protons. At 300 TeV iron primaries show a mean value $age/age(p)$ of 1.20 with a rms of 0.17 while the mean for protons lies at 1.00 as expected with a rms of 0.15.

EAS of different nuclei can also be distinguished by their lateral shower developments as measurable by comparing the number of Cherenkov photons within and beyond 100 m core distance. Unfortunately it is very difficult to measure the low density Cherenkov light up to a few hundred meters distance from the shower core with great precision. However using the energy reconstruction methods developed in this paper an indirect measurement of the light beyond 100 m is possible: if the energy is reconstructed only with Cherenkov light an E/A dependent correction (eq. 5) has to be applied to take into account the changing fraction of Cherenkov light measurable below 100 m and the fraction of the primary energy deposited in the electromagnetic cascade. Only the latter point has to be corrected if the energy reconstruction is done with the help of Ne (eq. 3). Therefore omitting all E/A corrections in both energy reconstruction methods (resulting in $E^*(Cl)$ and $E^*(Ne)$) and then comparing $E^*(Cl)/E^*(Ne)$ provides an indirect estimation of the amount of Cherenkov light at large distances. This is equivalent to compare the number of Cherenkov photons between 20 and 100 m core distance to Ne taking into account the distance to the shower maximum and density effects for the production of Cherenkov light. In Figure 8 (right) the energy ratios are plotted. A clear separation is visible for 300 TeV showers. An analysis of the chemical composition can profit from measuring the

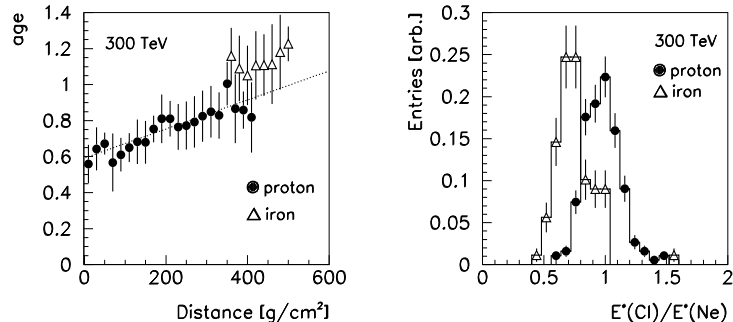


Figure 8: The age values as a function of the distance to the shower maximum (left), and the ratio of the energies reconstructed only with Cherenkov light and by using Ne and $slope$, where all corrections depending on E/A were omitted (right). Proton and iron showers of 300 TeV are displayed.

lateral extent of the electromagnetic cascade of an EAS at energies below approximately 1 PeV. At higher energies the lateral extensions no longer depend on the primary mass in a measurable way. With the observables used in this paper the chemical composition around the “knee” can only be derived from the longitudinal shower development.

8.3 Chemical Composition from a combined Analysis of the longitudinal and lateral Shower Development

The sample of 300 TeV showers was used to compare the sensitivity of the different parameters discussed in the last two sections on the mass of the primary nucleus. If cuts in different quantities are applied so that 90% of the iron showers are selected the following fractions of proton shower remain:

- Cut in $\log_{10}(A)$: 20%,
- cut in $age/age(p)$ or $E^*(Cl)/E^*(Ne)$: 40%.

The most sensitive parameter is derived from the longitudinal shower development, but also a discrimination between heavy and light nuclei can be derived from the lateral shower

extensions. To combine the information from the longitudinal shower development and the two comparisons referring to lateral extension of the EAS the probability densities for observing a specific $\log_{10}(A)$, $E^*(Cl)/E^*(Ne)$ or $age/age(p)$ value were parameterized for primary p, α , O and Fe nuclei of 300 TeV from the MC library. Following equation 8 (similar for other primaries than iron) a combined probability is calculated:

With $\rho_{Fe} = \text{prob}(\log_{10}(A), Fe) \cdot \text{prob}(E^*(Cl)/E^*(Ne), Fe) \cdot \text{prob}(age/age(p), Fe)$

$$\text{prob}(Fe) = \frac{\rho_{Fe}}{\rho_p + \rho_\alpha + \rho_O + \rho_{Fe}} \quad (8)$$

Table 3 lists the fractions for nuclei of different masses which are obtained by selecting 90% or 50% of all proton or iron showers. Clearly an analysis of the chemical composi-

Primary	Sel. 90% p	Sel. 50% p	Sel. 90% Fe	Sel. 50% Fe
Proton	90%	50%	8%	<1%
Helium	80%	17%	12%	1.5%
Oxygen	43%	3%	60%	24%
Iron	5%	<1%	90%	50%

Table 3: The remaining fraction of primaries with energies of 300 TeV after selecting 90% or 50% of the proton (iron) showers with cuts in $\text{prob}(p)$ or $\text{prob}(Fe)$.

tion improves if measurements of the longitudinal and lateral shower developments are combined. Light and heavy particles can be separated rather well. However with the four observables used here primary nuclei with masses similar to oxygen can be separated only in a statistical sense but not on an event by event basis. It seems to be difficult to distinguish between primary protons and α particles.

8.4 Systematics

Studies of systematic effects related to the CORSIKA code (stepwidth of the EGS part), atmospheric transmission, the fragmentation of the primary nucleus and the influence of different models to simulate the high energy interactions of the CR will be described in a forthcoming publication. In general the observables analyzed here show up to be much less model dependent than hadronic shower properties or muon distributions, mainly because the development of a shower behind its maximum determines the Cherenkov light and particle measurement, as considered throughout this paper.

9 Summary and Conclusions

In this paper methods were presented to determine energy and mass of charged cosmic rays from ground based observations of the electromagnetic cascade of air showers. From the slope of the lateral Cherenkov light density in the range of 20 to 100 m core distance the position of the shower maximum can be inferred without knowledge of the nucleon number of the primary particle. This leads to an unbiased determination of the energy per nucleon and, combined with the shower size at detector level or the number of registered Cherenkov photons, to a measurement of the primary energy. Thus a measurement of

the energy spectrum and a coarse determination of the chemical composition are possible without any a priori hypotheses.

With the observables considered in the present paper the energy resolution for primary nuclei is limited to approximately 30% at 300 TeV improving to 10% at 5 PeV due to natural fluctuations in the shower development. Further improvements of these results are only possible if accurate measurements of the non electromagnetic components of EAS are added.

At energies below 1 PeV, where results from EAS measurements can be compared to direct data from balloon flights, the sensitivity of the analysis of air showers by observing Cherenkov light and particles at detector level can be substantially improved by combining the results related to the longitudinal shower development with parameters derived from the lateral extension. This allows detailed tests of the described method to determine the chemical composition and the energy spectrum of cosmic rays.

One main characteristic of deriving energy and mass of primary nuclei from observations of the electromagnetic component of extensive air showers with the observables used here is the fact, that it are mainly the longitudinal shower development behind the shower maximum, the number of particles at the maximum and the penetration depth of the shower until it reaches the maximum, which determine the results. While the first two items do not vary much for different models describing the development of air showers the last item is more model dependent. In order to achieve results being as model independent as possible it is very desirable to combine the method described in this paper with complementary measurements. Analyses of the early stage of the shower development, of the hadronic component of EAS or detailed studies of the shower core may be considered for this purpose.

ACKNOWLEDGMENTS

The author would like to thank the HEGRA members for their collaboration. Especially I am very grateful to V. Hausteine, who performed most of the MC simulations and determined the chemical composition of CR with a different technique, to G. Heinzemann for many detailed, constructive proposals and improvements as well as for his general support, and to R. Plaga, who pioneered the analysis of charged CR in the HEGRA collaboration, for motivations and detailed discussions. Special thanks to the authors of CORSIKA for supplying us with the simulation program and their support. I thank Gerald Lopez for his careful reading of the text and for providing valuable suggestions. This work was supported by the BMBF (Germany) under contract number 05 2HH 264.

References

- [1] Aharonian, F., et al. (HEGRA collab.), 24th ICRC Rome **1**, 474 (1995)
- [2] Kamata, K. and Nishimura, J., Prog.Theoret.Phys., Suppl **6** (1958)
Greisen, K. Ann.Rev.Nucl.Sci.**10**,63 (1960)
- [3] Capdevielle, J.N. et al., KfK Report **4998** (1992)
Knapp, J., Heck, D., KfK Report **5196B** (1993)
- [4] Hausteine, V., doctoral thesis at Univ. of Hamburg (1996), in preparation
- [5] Patterson, J.R., Hillas, A.M., J.Phys.G.**9**,1433 (1983)
- [6] Gabriel, T.A., et al., Nucl.Instrum.Meth.**A338**,336 (1994)